Czesław Machelski
Prof. dr hab. inż.
Politechnika Wrocławska, Wydział Budownictwa Lądowego i Wodnego;
Katedra Mostów i Kolei
czeslaw.machelski@pwr.edu.pl

Leszek Korusiewicz
Dr inż.
Politechnika Wrocławska, Wydział Mechaniczny; Katedra Wytrzymałości materiałów
leszek.korusiewicz@pwr.edu.pl

DOI: 10.35117/A_ENG_18_12_10

Investigations of contact interactions in buried corrugated metal structure by means of strain gauges

Abstract: This paper analyzes the distributions of contact soil-steel interactions in the form of normal and shear components. Unit strain measured by electrical resistance strain gauges are used in the calculations. An algorithm for transforming strain functions into contact forces distributed along the circumferential section of the steel shell is presented. When the measuring points are regularly spaced, it is advantageous to adopt the differential approach to the solution. The effectiveness of the algorithm has been demonstrated through a test conducted in laboratory conditions, using a static force system as the rolling stock load. The intensity of loading from the standard value to the predicted limit value was adopted as the variable parameter in the analysis. The results of the calculations are presented in the form of functions of the forces distributed along the shell's circumferential section. An analysis of three exemplary cases, carried out in this paper, has shown that even when the load distribution on the soil surcharge is almost uniform, the contact forces form composite functions. Moreover, the latter considerably diverge from load proportionality.

Keywords: Buried corrugated metal structures; Contact interactions; Static loads; Tensometric measurements; Laboratory tests

Contact interactions in buried corrugated metal structure

A characteristic feature of buried corrugated metal structures, in contrast to classical bridges, is the high impact of ground backing and road surface as bearing elements [10]. The stiffness of the corrugated metal coat itself is small. When laying the backfill, it is subject to considerable deformation because it is a geometric form limiting the filling of the ground in the bridge facility. For this reason, it takes over the full pressure of the ground as well as the retaining wall (but susceptible). Only when surrounded by backfill, the coating becomes an effective element of the structure that allows the transfer of significant, communication loads.

Three groups of tests are used to map the interaction of the coating with the soil in the contact layer of buried corrugated metal structure:

a. displacement of the coat points, allowing to determine the deformation of the perimeter band [6, 7, 9];
b. unit deformations of corrugated sheet, used to determine internal forces in the perimeter of the coating [4, 5];
c. direct measurement of soil pressure on the coating [12, 13].

In each of these measurement groups, a different research methodology is implemented. However, as a result, contact effects can be obtained in the form of surface forces, usually distributed into two components: normal p and tangent t, as in Fig. **1**.

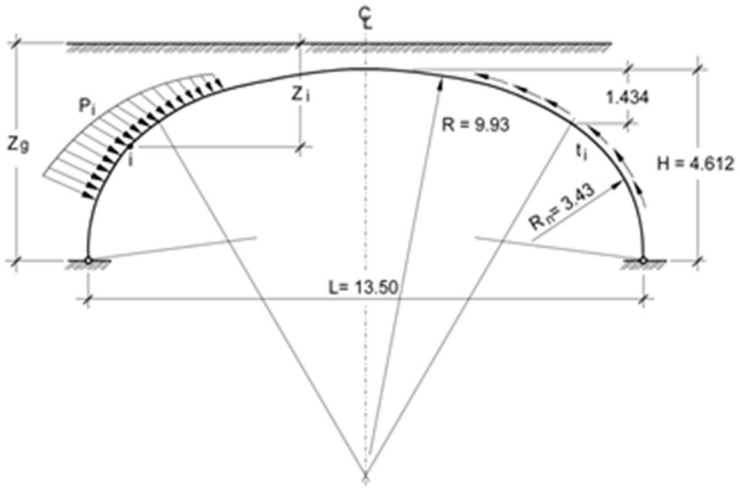

1. Diagram of contact forces during building construction [3]

During construction, the method a. Is effective. The result of soil interactions is the deformation of the coating defined as displacements of measurement points in the form of vertical components in and horizontal *u*. Measurements are carried out using geodetic techniques - sufficiently accurate due to high displacement values [8]. On the basis of dependence displacement - contact interaction, in the model of the peripheral band of the shell as a component separated from the structural system, the components of normal *p* and tangential *t* forces are calculated.

The effects of soil on the coating are variable during construction as well as during exploitation. The value of internal forces is mainly influenced by the position of the analyzed point in relation to the level z_g. However, besides the physical features of the soil, the technology of compacting the backfill, its thickness on both sides of the coating, the equipment used, climatic conditions, and work breaks are of significant importance. These effects with random features are mapped in the shell's deformation - they are a record of the object's construction process. On the basis of post-construction displacement, the quality of works in these facilities is assessed. For coatings with a distinct geometry, a displacement forecast is prepared - analogously to the concrete bridge compression program.

In the case of functional loads, the method b discussed at work is effective. It is particularly useful when there is a regular spacing of the measuring sensors (strain gauges) on the perimeter of the coating. In this work, the immediate effect of the load, treated as static, is analyzed. The results of these analyzes can be used to assess the effectiveness of classic geotechnical models [1, 2, 3, 11].

Direct measurement of soil pressure, used in process c (using pressure gauges), does not require modeling of the soil's influence on the coating [13]. It can be used to observe changes in the interaction between soil and coating in the facility during its operation. Figure **2** shows one example of the object research results in Dovre (Norway). The coating was made as a horizontal ellipse with a span L = 10.78 m and a height H = 7.13 m with a 4.2 m thick name. The coating was made of a corrugated sheet with a typical profile of MP 200 × 55 × 7. In the corners of the shell concrete stiffening ribs in the shape of a triangular cross-section were made, shown in Fig. 2.

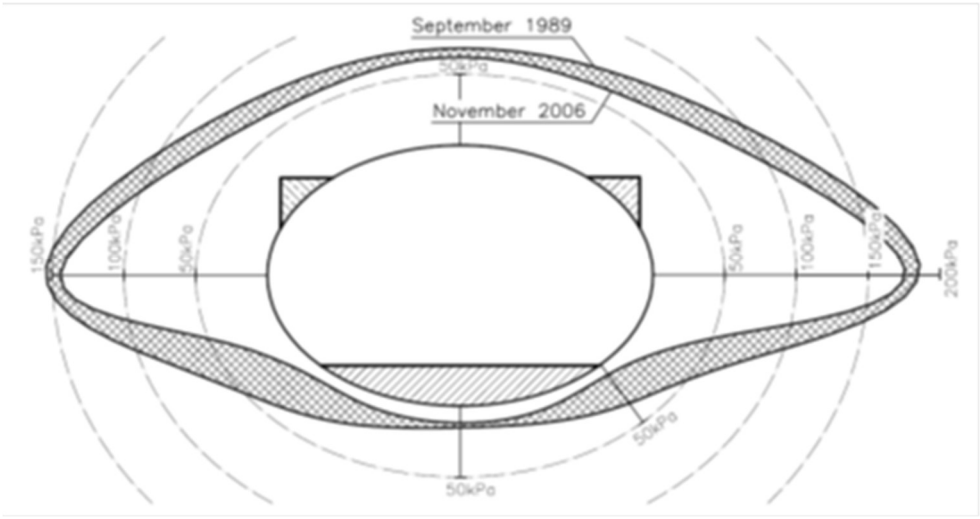

2. Change of the soil's influence on the coating during the lifetime of the object [7]

The largest values of the normal component of p interaction were obtained at a depth of 7.8 m from the level of the roadway (subgrade). In the summary of test results from these measurements [12], a 30% reduction in pressure on the coating after twenty-one years of use was found. In this measuring technique, it is difficult to determine tangent forces. The disadvantage of the measuring system is interference in the ground center.

In the FEM calculation models, ground and coat objects [11] are distinguished by two structural subsystems: corrugated metal shell and the remaining part in the form of ground backfill, road surface, and road foundation. The second subsystem is difficult to identify. Therefore, determining the mutual interactions of the soil with the coating allows the object model to be reduced to a separate perimeter band. The results given in the paper can also be used to model the interaction of contact between the coating and the soil.

Description of the tested structure

The analyzed model of the object with a ground-shell structure, as in Fig. **3a** was built at the Research Institute of Roads and Bridges in Żmigród. The Multiplate coating was made of corrugated sheets MP 150 × 50 × 3.75 mm with a closed profile and shape as in Fig. **3b**, length L = 14.4 m.In the tests of deformation and internal forces of the coating, the measurement base shown in Fig. 4 was used. On the chosen central perimeter band, electrofusion strain gauges were glued onto the corrugated metal sheet available from the inside. A regular distance between the strain gauges 2b = 0.631 m was applied. At each measurement point, the sensors were arranged in pairs, at the top and the crank valley, located in the circumferential direction.

A wide range of static and cyclic load variants was applied in the general testing program for the culvert model. The research of the facility was carried out at several thickness levels and various load schemes. The results of the tests presented in the paper concern the minimum thickness of the backfill, i.e. the level of h = 0.6 m in the shell key. The loads simulating the rolling stock were selected as the standard UIC 71 scheme for the design of bridge structures. The system of load forces with a total P-value between the actuators and the tested model was laid out using two layers of railway sleepers and a steel plate arranged on them, as in Fig. 3a. In the selection of force P, the dynamic coefficient for a given value of h was taken into account. The paper presents selected results from one measurement system, hereinafter referred to as:

scheme A starting a series of loads with a force P = 586 kN;
scheme B third, subsequent load as in scheme A;
scheme C maximum load with a force P = 1500 kN.

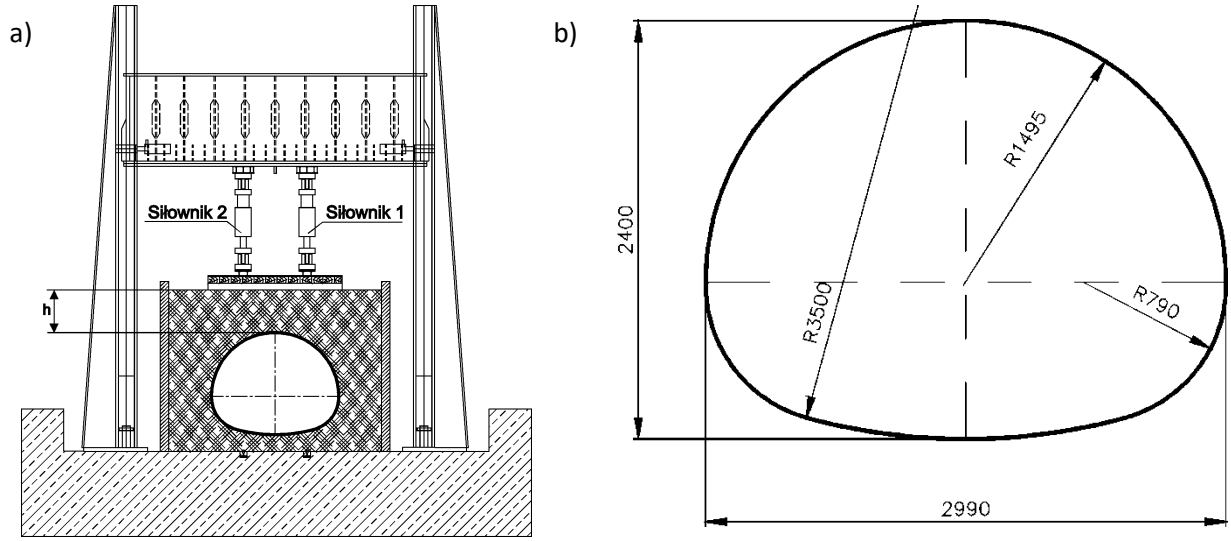

3. Scheme of the test bench and geometry of the peripheral coating band

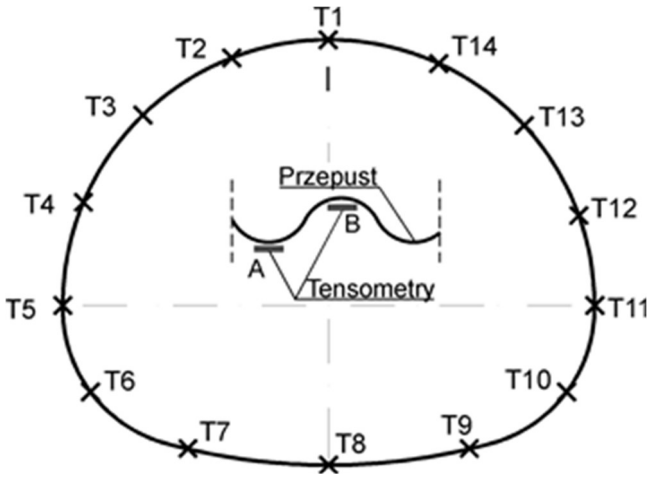

4. Scheme of arrangement of extensometers on the perimeter of the coatin

The dependence of the shell deformation - the effect of the soil

The twin sensor system, assuming the principle of flat cross-sections, makes it possible to determine the deformations in the axis of inertia of the corrugated sheet cross-section as in dependence

$$\varepsilon_O = \frac{\varepsilon_A(f-t)+\varepsilon_B(f+t)}{2f}. \tag{1}$$

The formula (1) includes the corrugated metal sheet MP a × f × t. In the analyzed case, the sheets have the following dimensions: MP 150 × 50 × 3.75 mm. To determine the change in the radius of the curvature of the shell, the geometrical relationships of the sheet and ε_A and ε_B can be used as in the equation

$$\rho = \frac{\varepsilon_A - \varepsilon_B}{f}. \tag{2}$$

The geometric quantities determined in (1) and (2) are used to determine the internal forces in the coat: axial force

$$n = \frac{E \cdot A}{a} \varepsilon_0 \tag{3}$$

and bending moment

$$m = \frac{E \cdot I}{a} \rho \tag{4}$$

where: A/a = 4,70 mm^2/mm and I/a = 1432,6 mm^4/mm they are geometrical characteristics of the corrugated metal cross-section (wavelength a) while E = 20,000 MPa is the strength feature of the material (steel).

From static dependencies of internal forces n and m as a function of the distance between points, but counted along the peripheral band of the shell as a circle segment with chord length b, we obtain in a differential manner the normal interaction

$$p_j = \frac{m_i - 2m_j + m_k}{b^2} + \frac{n_j}{R} \tag{5}$$

and tangents

$$t_{jk} = \frac{n_j - n_k}{b} + \frac{m_j - m_k}{b \cdot R}. \tag{6}$$

The p_j value is calculated in the j-point measurement point, while the t_{jk} forces between j and k points as in Fig. 5. In this work, to increase the accuracy of the graphs, additional intermediate points between the measurements were introduced, as in Fig. **4**. Hence the length The curves between the measurement points are 2b = 0.631 m. In formulas (5) and (6) the radii of the R coating on the length of the perimeter band are varied (R = 1.495 m in the upper part, R_n = 0.79 m in the corner section and R_d = 3, 50 m at the base).

The following geometric relationships result from the shell section as in Fig. **5**: the distance between the measurement points (2C - chord length)

$$C^2 = F(2R - F) \tag{7}$$

and the arc length between the measuring points

$$2b = 2\varphi \cdot R \tag{8}$$

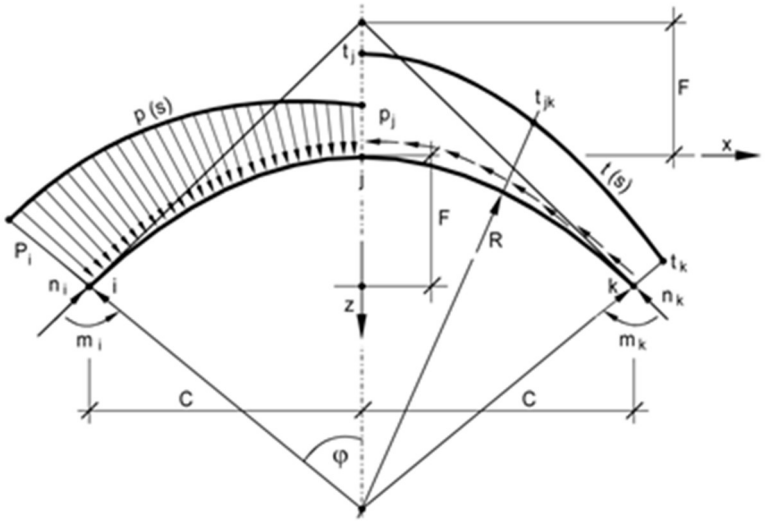

5. Determination of internal forces and soil effects on the coating

Intensity of contact interactions

In Figures **6-11**, the value of s is the distance of the analyzed section from the key of the coat but counted along the band of the peripheral shell (when s = 0 point is located in the axis of sym-

metry of the structure T1). Thus, the distances of the measuring points on the left side of the coat are negative, with values

$$s_i = -2b(i-1) \text{ [m]} \quad (9)$$

when i is the number of the measurement point, as in Fig. 4, and 2b = 0.631 m. In the drawings given in this chapter, it was assumed that the negative values are the left part of the coat (T1 - T8) and the positive its right side (T14 - T8).

The form of all the graphs given in the work shows a slight shift in the results of measurements with reference to the symmetry axis of the shell. For this reason, the diagrams, with the assumed load symmetry, are slightly different on the left and right side of the peripheral band. The charts below show characteristic locations away from the shell key. When s = 8b = ± 2.52 m, the results relate to points T5 and T11 located at the level of the spread of the shell L. Values of s = 4b = ± 1.26 m correspond to the points T3 and T13 of the coat.

Scheme A applies to measurements initiating the load cycle in the same measurement system (but not the first in the entire test program). The key has maximum negative bending moments, but in a few other places moments with similar values are created (also negative and positive). In the m(s) and n(s) graphs, a characteristic place is visible when $\varphi = 45^o$ so $s = \pi R/4 = \pm$ 1,17 m, in which the highest values of internal forces in the shell occur. From the interaction diagram of normal p, the offset of the load system is visible in relation to the symmetry (by design) of the shell. The distance between the maximum normal impacts p (s) is approx. S = 8b = 2.52 m

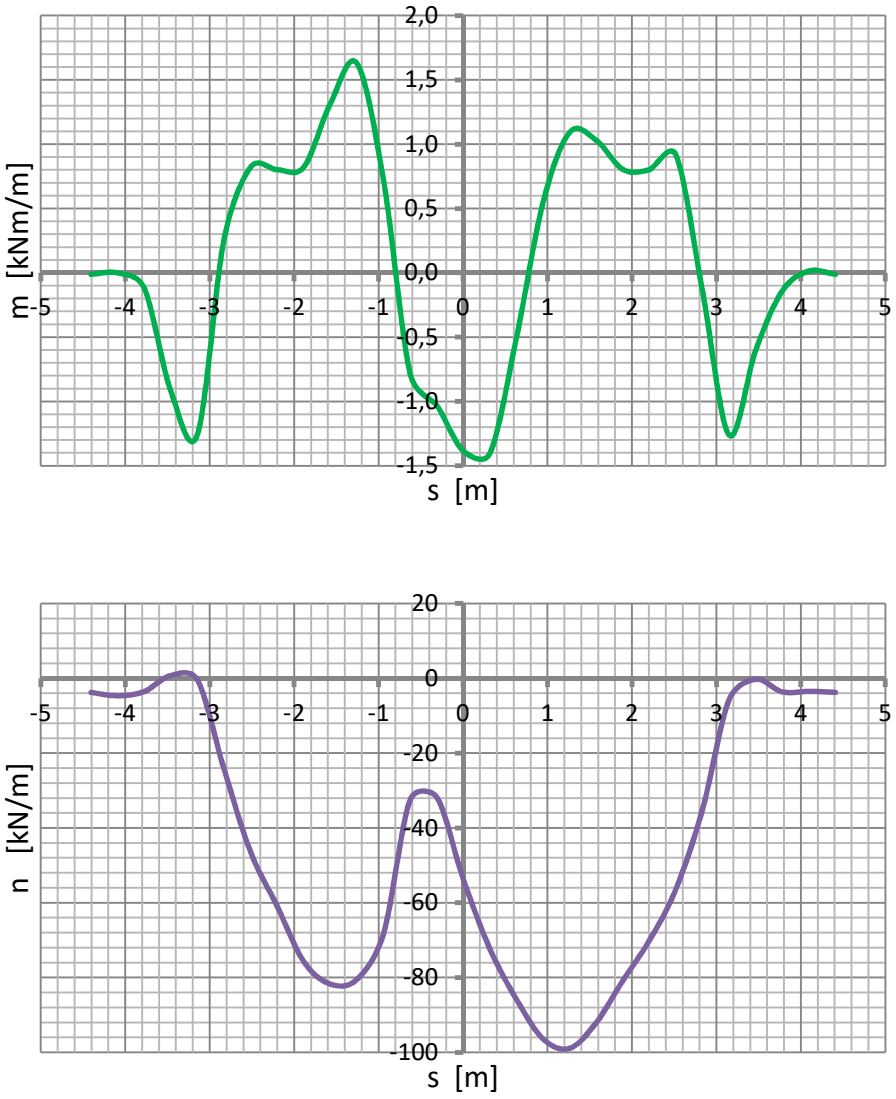

6. Internal forces in the perimeter band of the shell in scheme A

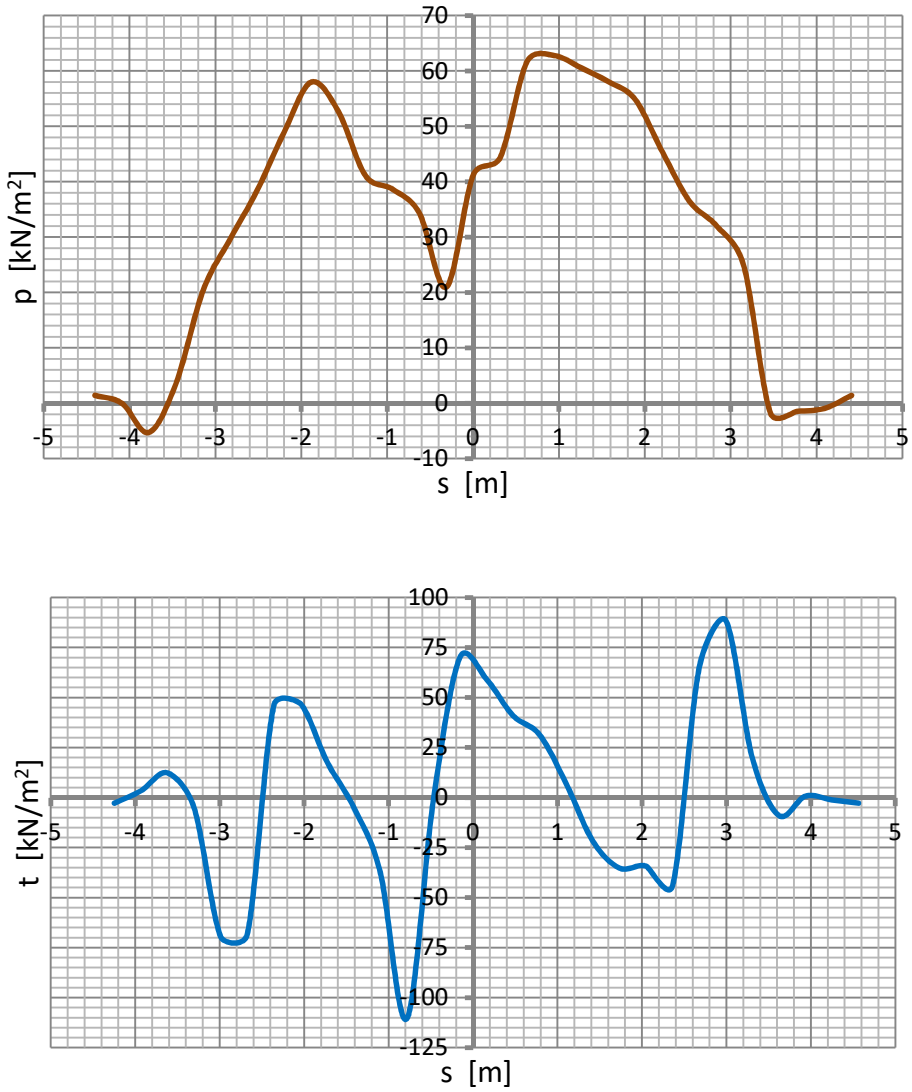

7. The effects of soil on the length of the peripheral coating band in Scheme A

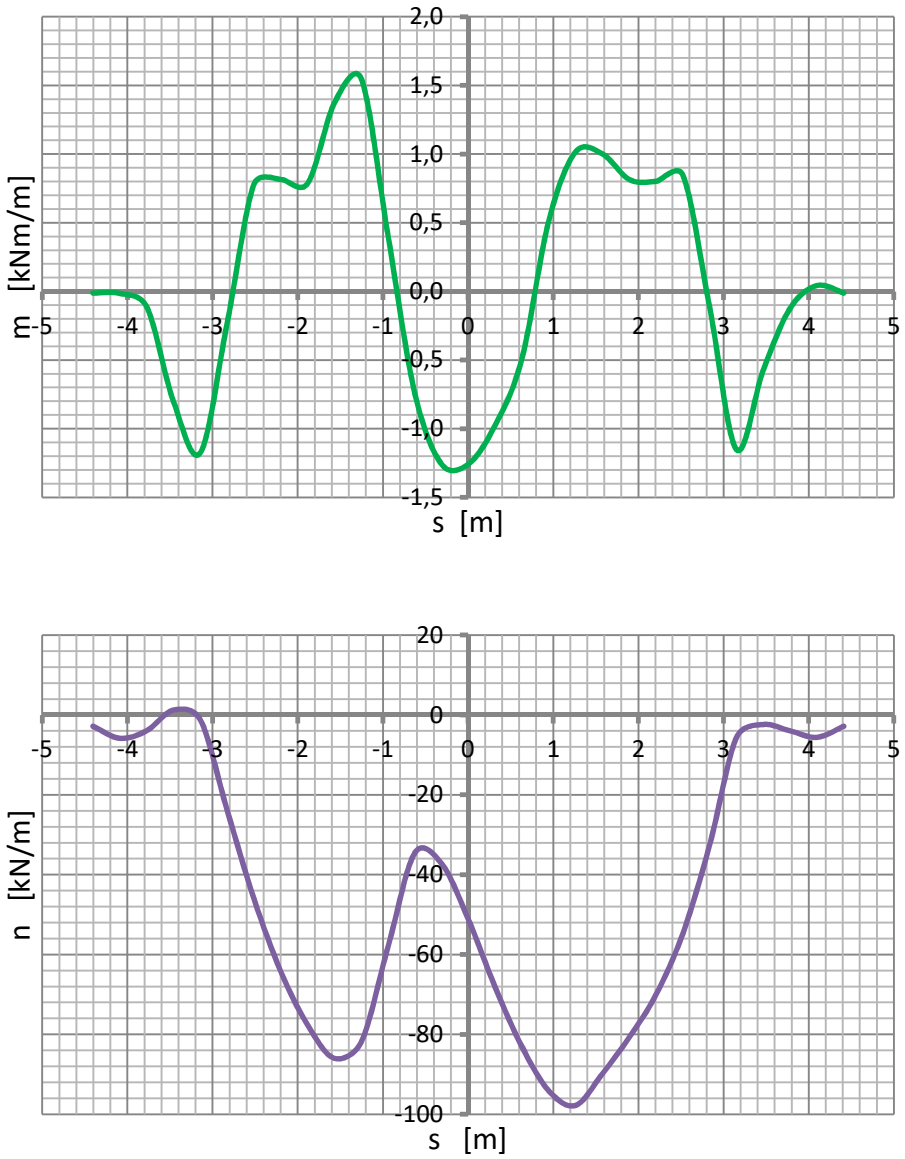

8. Internal forces in the perimeter of the shell in scheme B

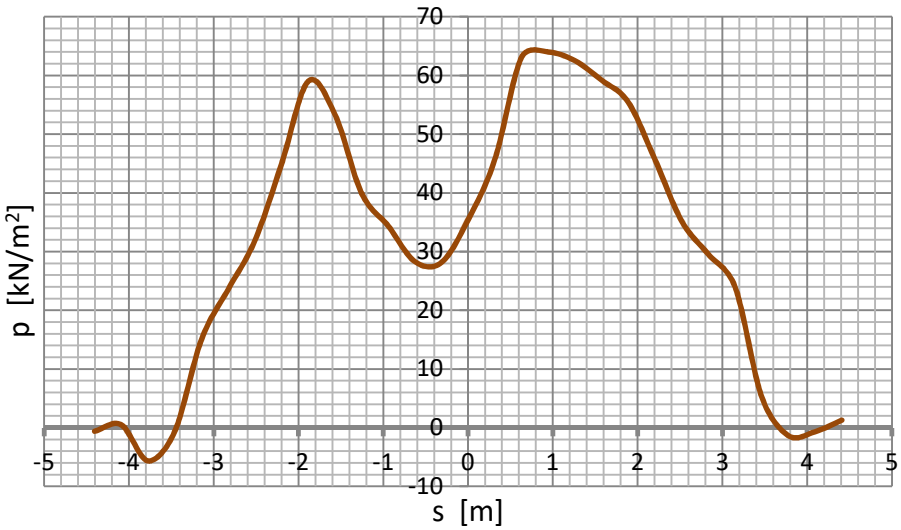

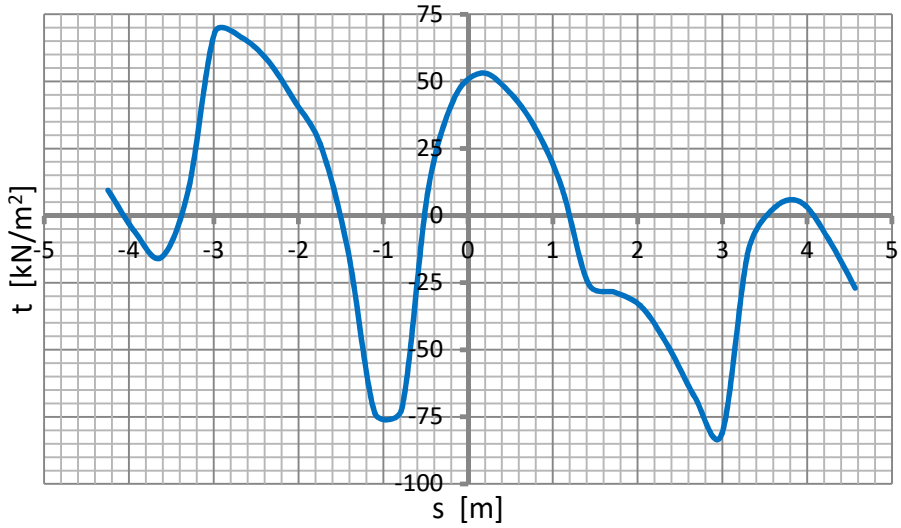

9. The effects of soil on the length of the peripheral coating band in scheme B

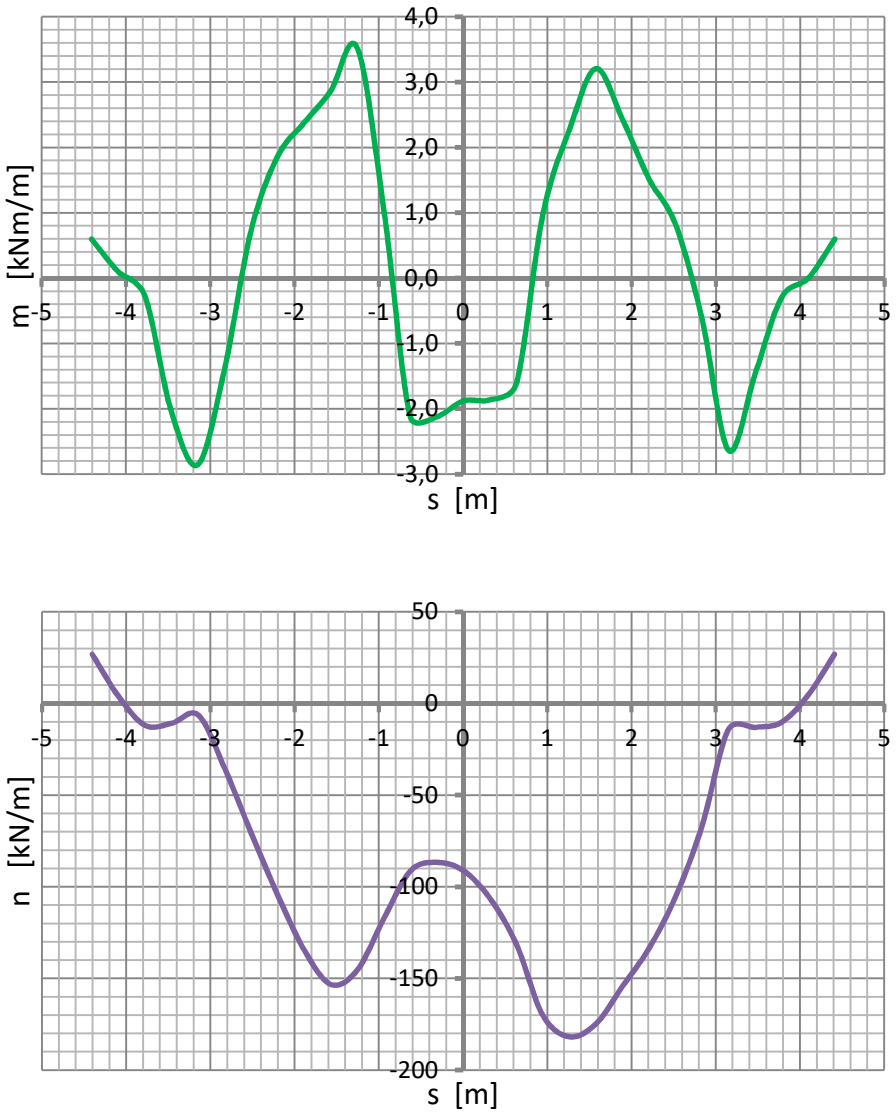

10. Internal forces in the perimeter of the shell in scheme C

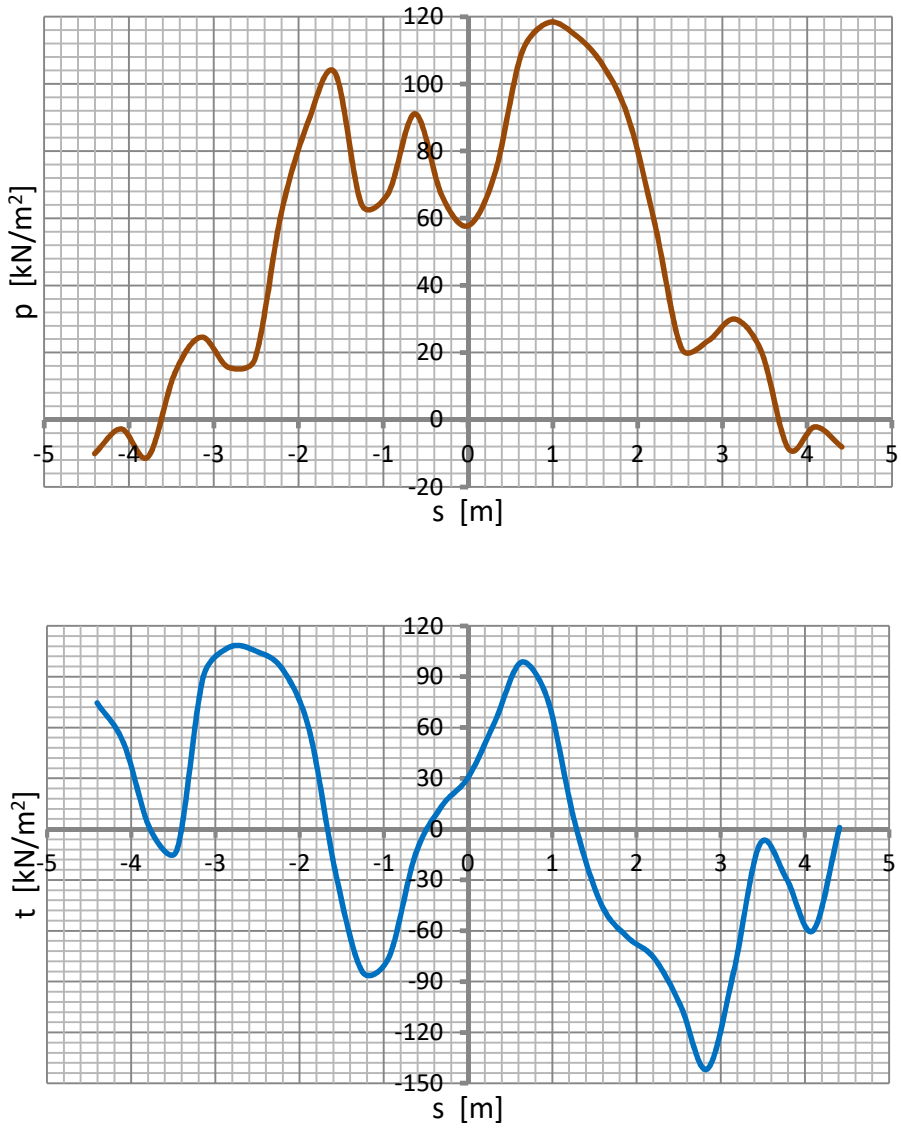

11. The effects of soil on the length of the peripheral band of the coating in scheme C

Scheme B applies to measurements obtained in the third cycle of the load as in scheme A. Analogous graphs of internal forces indicate the constancy of the structure system. In the case of tangential forces t(s), a significant difference is visible on the right side of the shell - change of the sign in the zone of points T10 - T1 (as in Figures 7 and 9).

Scheme C was important in assessing the safety of the object, because the load (P strength) was increased by 1500/586 = 2.56 times in relation to the norm value as in scheme A. Table 1 compares the maximum values obtained in the analyzed load schemes marked as C/A. The largest increase was obtained in the case of bending moments m, in principle similar to the proportion of load change. The axial forces n, much like the normal interactions p, increased much less by half the increment of the load. On the other hand, the tangent forces t remained almost unchanged and with a similar distribution as in scheme B. Thus, the soil's influence on the coating does not change proportional to the load.

Tab. 1. Comparison of extreme values of internal and contact forces

Load scheme	Analyzed static units			
	m [kNm/m]	*n* [kN/m]	*p* [kN/m^2]	*t* [kN/m^2]
A	1,63	98,9	62,8	-110,4
B	1,55	97,8	60,8	-81,3
C	3,53	181,8	117,9	-129,5
C/A	2,17	1,84	1,88	1,17

Figures **6-11** present the results of examination of an object with natural dimensions and a mobile (railway) load of a standard value in the form of a P. force system. In the examined object (and the tested) the ground impacts from the own weight (ground fill and surface) are added with the effect of external load. In the values of normal interactions p(P), given in the graphs, the ground pressure $p(z_g)$ generated during the filling of the backfill was not taken into account, as in Fig. **1** and the weight of the load transfer structure, as in Fig. **2b**. For this reason, the tangent interactions t (P) given in these graphs may be equivalent to p(P), and the proportion $(t(P)/p(P+z_g)$ does not mean that the coefficient of friction of the ground against the coating is exceeded

Fig. **12** presents a graph of the resultant impact of soil on the coating calculated on the basis of p and t components, as in the formula

$$q = \sqrt{p^2 + t^2} \tag{10}$$

for graph C. From the graph q (s) an almost uniform impact distribution is visible in the range -2.8 <s <2.9 m, that is in the range of points T5 - T1 - T11 (as in Fig. **4**).

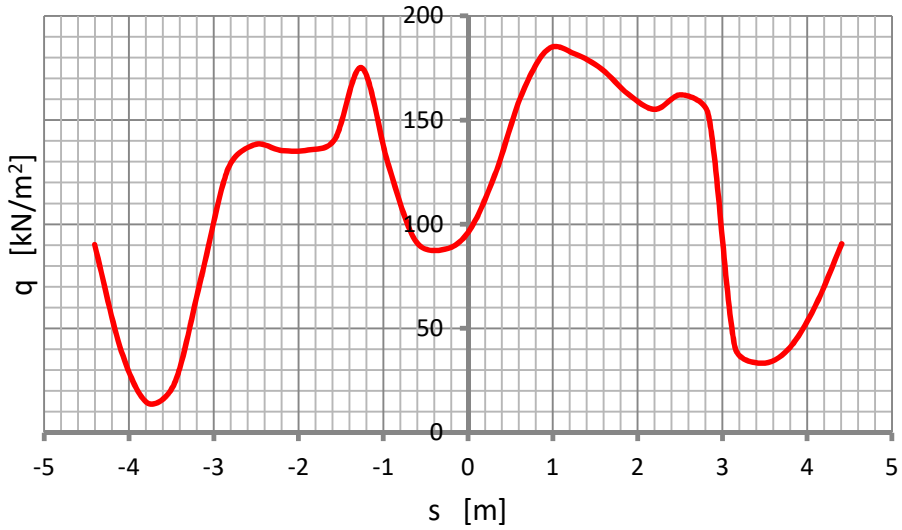

12. Resultant soil effects on the length of the peripheral band of the coating in scheme C

Summary

During tests at the breaking load in the coating, the maximum stress σ = 96.4 MPa at point T3 was obtained. At the standard load, σ = 47.4 MPa was obtained, i.e. half of the previous value. The values of these stresses are significantly lower than the strength of the corrugated steel sheet S235JRG2. In general, in objects subject to exploitation - with a larger spread, stresses from utilization loads are much lower.

The functions of soil interactions on the p(s) and t(s) coatings depend on the location of the system of forces on the plane of the level and their distribution by the (railway) surface. Normal interactions p(s) assume a uniform form as to the sign but with a complex shape resulting also from the geometry of the peripheral band of the shell, i.e. the radii of curvature, as in Fig. 3b.

The comparison between the n(s) and p(s) graphs shows their high similarity. The bending, as in the pattern, is also important for p(s) (5).

The results of the analyzes given in the paper indicate a high share of tangential loads t(s) in the effect of soil on the coating. This is important in the case of mapping the contact layer in the construction modeling in MES. In the shape of these graphs, the influence of the geometry of the peripheral band of the shell, i.e. the radii of curvature, as in the formula (6), but also the scheme of the load on the nails is visible. The values of t(s), often exceeding p(s), are important in the functions of internal forces in the shell n(s) and m(s). The effects of soil on the coating do not change proportional to the load.

Source materials

[1] *Bakht B.:* Evaluations of the design methods for soil-steel structures in Canada. Archives of Institute of Civil Engineering, No 1/2007, pp. 7-22.

[2] *Jaske T., Przedecki T, Rossiński B.:* Mechanika gruntów. Państwowe Wydawnictwo Naukowe, Warszawa 1966.

[3] Klöppel K., Glöck D.: Theoretische und experementelle Untersuchungen zu den Traglast problemen bigeweicher in die Erde ein gebetteter Rohre. Veröffenntlichung des Instituts Statik und Stahlbau der Technische Hochschule Darmstadt, 3/1979, H-10.

[4] *Korusiewicz L.*, *Chruścielski G.*, *Jasiński R.:* Practical aspects of strains, stresses and internal forces estimation during field and laboratory tests of corrugated culverts. Archives of Institute of Civil Engineering, **12**, 2012, pp. 117-131

[5] *Korusiewicz L.*: Badania w czasie zasypywania gruntowo-powłokowej konstrukcji o dużej rozpiętości wykonanej bez dodatkowych elementów usztywniających. Roads and Bridges – Drogi i Mosty, **14**, 3, 2015, s. 203-218

[6] *Machelski C.*: Estimation of internal forces in the shell of soil-steel structures on the basis of its displacements during backfilling. Studia Geotechnica at Mechanica, 1/2009, pp. 19-38.

[7] *Machelski C.*: Oddziaływania pojazdu na powłokę w obiektach gruntowo-powłokowych. Przegląd Komunikacyjny, 9/2017, s. 5-10.

[8] *Machelski C.*: Skuteczność pomiarów geodezyjnych podczas budowy obiektów gruntowo-powłokowych. Mosty, 8/2016 s. 24-28.

[9] *Machelski C.*: Szacowanie oddziaływania zasypki na powłokę w obiekcie gruntowo-powłokowym na podstawie deformacji powłoki. Przegląd Komunikacyjny, 11/2016, s. 31-36

[10] *Machelski C.*: Sztywność obiektu mostowego jako parametru użytkowego konstrukcji inżynieryjnych. Przegląd Komunikacyjny, 2/2016, s. 27-32.

[11] *Szajna W.S.*: Numerical model for the analysis of construction process of soil-steel culverts. Archives of Institute of Civil Engineering, No 1/2007, pp. 215-223.

[12] *Vaslestad J., Kunecki B., JohansenT. H.*: Twenty one year pressure measurements on buried flexible steel structure. Archives of Institute of Civil Engineering, No 1/2007, pp. 233-244.

[13] *Vaslestad J.*: Long-term behaviour of flexible large-span culverts, Publication No.74, Norwegian Pub. Roads Administration, Oslo 1994, pp. 38-56.